Electrogenerated Thin Films of Microporous Polymer Networks with Remarkably Increased Electrochemical Response to Nitroaromatic Analytes

Alex Palma-Cando and Ullrich Scherf*

Macromolecular Chemistry Group, Bergische Universität Wuppertal, Gaußstraße 20, D-42119 Wuppertal, Germany

S Supporting Information

ABSTRACT: Thin films of microporous polymer networks (MPNs) have been generated by electrochemical polymerization of a series of multifunctional carbazole-based monomers. The microporous films show high Brunauer−Emmett−Teller (BET) surface areas up to 1300 $m^2 g^{-1}$ as directly measured by krypton sorption experiments. A correlation between the number of polymerizable carbazole units of the monomer and the resulting surface area is observed. Electrochemical sensing experiments with 1,3,5-trinitrobenzene as prototypical nitroaromatic analyte demonstrate an up to 180 times increased current response of MPN-modified glassy carbon electrodes in relation to the nonmodified electrode. The phenomenon probably involves intermolecular interactions between the electron-poor nitroaromatic analytes and the electron-rich, high surface area microporous deposits, with the electrochemical reduction at the MPN-modified electrodes being an adsorption-controlled process for low scan rates. We expect a high application potential of such MPN-modified electrodes for boosting the sensitivity of electrochemical sensor devices.

KEYWORDS: microporous materials, electropolymerization, thin films, electrochemical reduction, nitroaromatic analytes
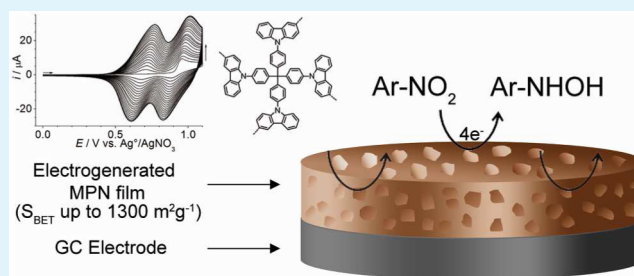
INTRODUCTION

Microporous polymer networks (MPNs) have been often related to potential applications for gas capture[1,2] and separation,[3,4] catalysis,[5−7] organic electronic devices,[8,9] and solid state sensors.[10] For the latter two applications, the availability of high quality films is required.[11] The chemical methods, which are commonly used for MPN generation, usually produce powdery and practically intractable samples.[12,13] The possibility of an electrochemical generation of carbazole-based MPN films has been recently demonstrated.[14,15] The resulting electrochemically generated MPN films have been used as electrode interlayers of organic electronics devices such as organic light emitting diodes and organic solar cells or as an electrode material of supercapacitors.[16] A direct proof for the microporosity and high surface area of such films has been first presented in a recent publication by Jiang and co-workers[17] in krypton gas sorption measurements followed by data analysis based on the Brunauer−Emmett−Teller (BET) equation. On the other hand, films of carbazole-based polymers have been used as sensors for nitroaromatic compounds (NACs) via fluorescence quenching[18] or electrochemical reduction.[19] The latter principle is based on the quantification of the cathodic current which is produced during reduction of the nitroaromatic analytes. Zhang and co-workers used films of electropolymerized, carbazole-based monomers for the electrochemical detection of NACs. However, their monomers contain

flexible alkylene linkers and should not form microporous networks. Therefore, the novelty of our approach is to combine permanent microporosity of electrochemically deposited films with the electrochemical detection of nitroaromatic analytes.

Within this work, we report the electrochemical generation of MPN films starting from a series of multifunctional carbazole-based monomers, as well as direct porosity measurements of the resulting films by the krypton sorption method. The extracted BET surface area data are compared to the S_{BET} values of corresponding, chemically synthesized bulk MPNs which are obtained as powders. Increased functionality of the multifunctional carbazole-based monomers causes increased BET surface areas, most probably due to an increased rigidity of the networks. Moreover, glassy carbon (GC) electrodes modified with our MPN films have been used for the electrochemical sensing of the prototypical nitroaromatic analyte 1,3,5-trinitrobenzene (TNB). Here, a correlation between the surface area of the MPN films and the cathodic current response to TNB is observed. The results demonstrate that modification of GC electrodes with microporous polymer coatings can boost the sensitivity to NAC by more than 2 orders of magnitude most probably driven by intermolecular

electronic interactions between the electron-poor nitroaromatic analytes and the electron-rich MPN surface. Finally, the electrochemical reduction of the nitroaromatic analytes on the MPN-modified GC electrodes is studied at different scan rates. The process is characterized as an adsorption-controlled phenomenon involving an adsorbate layer of the NACs for low scan rates (<0.075 V s^{-1}); the current is directly proportional to the scan rate. With increasing scan rate the process becomes diffusion-controlled, since the transport of the analyte molecules is now the limiting process, the current is now proportional to the square root of the scan rate for high scan rates (>0.075 V s^{-1}).

■ EXPERIMENTAL SECTION

Synthesis. 4,4′-Di(carbazol-9-yl)-1,1′-biphenyl (CBP), tri[4-(carbazol-9-yl)phenyl]amine (TCTA), and 1,3,5-tri(carbazol-9-yl)benzene (TCB) were purchased from commercial suppliers. Synthetic details for 4,7-di[4-(carbazol-9-yl)phenyl]benzo[c][1,2,5]thiadiazole (CBPBT), 2,2′,7,7′-tetra(carbazol-9-yl)-9,9′-spirobifluorene (SpCz), and tetra[4-(carbazol-9-yl)phenyl]methane (TPTCz) as well as the FeCl$_3$-mediated syntheses of all corresponding bulk polymers are reported in the Supporting Information. ^{1}H and ^{13}C NMR spectra were obtained on Bruker Avance 400 and III 600 machines. APLI mass spectra were recorded on a Bruker Daltronik microTOF system (KrF*-Laser ATLEX-SI, ATL Wermelskirchen). Nitrogen and krypton adsorption−desorption isotherms were recorded on a BEL Japan Inc. Belsorp-max system at 77 K. All samples were dried on a Belprep-vac II at 140 °C and ~2 Pa overnight prior to the sorption measurements.

Electropolymerization of Carbazole-Based Monomers and Electrochemical Reduction of Nitroaromatic Analytes. The 0.5 mM solutions of the monomers are prepared in acetonitrile/dichloromethane (1:4). Following, 0.1 M tetrabutylammonium perchlorate (TBAP) is added as supporting electrolyte. The solutions were placed in a three-electrode cell, attached to an electrochemical workstation PAR VersaSTAT 4 under argon atmosphere at 25 °C. A platinum disc (for monomer and polymer characterization), indium tin oxide (ITO, for thickness/roughness, and surface area measurements of the MPN films), and glassy carbon (GC, for electrochemical sensing of nitroaromatic analytes) were used as working electrode (WE), in combination with a platinum counter electrode (CE) and Ag°/AgNO$_3$ (0.1 M AgNO$_3$, 0.60 V vs NHE, nonaqueous reference) or Ag°/AgCl(sat.) (3 M NaCl, 0.21 V vs NHE, aqueous reference) as reference electrodes (REs). Potentiodynamic or potentiostatic regimes were applied for the generation of microporous films on the electrodes. Thick films on ITO were produced by applying an oxidative potential of 1 V (CBP, SpCz, and TPTCz) or 1.1 V (CBPBT, TCB, and TCTA) for 20 min. After polymerization a potential of 0 V was applied for 60 s in order to discharge the deposits. After rinsing and careful drying, the films can be used for krypton gas sorption measurements. Thin films on GC were produced by applying a potential of 1.1 V until an oxidative charge density of 25.5 mC cm^{-2} was accumulated. After polymerization a potential of 0 V was applied for 30 s in order to discharge the deposits. After rinsing, the MPN-modified GC electrodes were used as WE in 0.2 M KCl and 0.1 M PBS (pH 7.4, Ar atmosphere) at 25 °C. For detection of nitroaromatic analytes, linear scan voltammograms were recorded from 0 to −1 V with a scan rate of 0.01 V s^{-1}. For electrochemical reduction of 1,3,5-trinitrobenzene (TNB), nitrobenzene (NB), and 2,4,6-trinitrophenol (TNP, picric acid) aliquots from stock solutions in acetonitrile (for TNB and NB) or water (for TNP) were added to a buffered aqueous solution by adjusting the concentration of the nitroaromatic analyte from 0 to 100 μM. The AFM images were obtained with an atomic force microscope Bruker diInnova operated in the tapping mode; the surface roughness was extracted from topography images. The thicknesses of the films were measured with a surface profilometer Vecco Dektak 150.

■ RESULTS AND DISCUSSION

The six carbazole-based monomers were purchased from commercial suppliers or synthesized by us (see the Supporting Information). In our experiments, monomers with two, three, and four carbazole substituents have been used: 4,4′-di-(carbazol-9-yl)-1,1′-biphenyl (CBP), 4,7-di[4-(carbazol-9-yl)-phenyl]benzo[c]-[1,2,5]thiadiazole (CBPBT), tri[4-(carbazol-9-yl)phenyl]amine (TCTA), 1,3,5-tri(carbazol-9-yl)benzene (TCB), 2,2′,7,7′-tetra(carbazol-9-yl)-9,9′-spirobifluorene (SpCz), and tetra[4-(carbazol-9-yl)phenyl]methane (TPTCz) (Scheme 1).

Scheme 1. Chemical Structures of the Investigated Carbazole-Based Monomers: (a) CBP, (b) CBPBT, (c) TCTA, (d) TCB, (e) SpCz, and (f) TPTCz
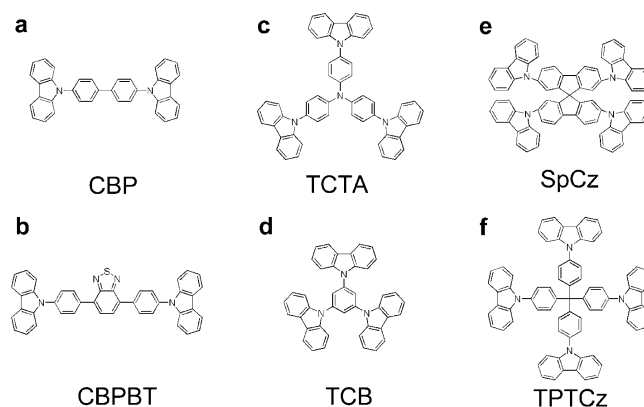
Electropolymerization of thiophene-,[20,21] pyrrole-,[22] and carbazole-based[23,24] monomers has been extensively studied due to the interesting properties of the resulting conducting polymer (CP) films, e.g., their electrochromic behavior.[25−27] Electrochemical oxidative coupling of carbazole was first described by Ambrose and Nelson.[28] Applying oxidative potentials, cation radicals are initially generated. Their dimerization and deprotonation lead to the formation of 3,3′-carbazole dimers. The initially formed dimers can undergo further oxidative coupling reactions.

Until now the majority of research into CPs has been focused on the synthesis of linear polymers. However, three-dimensional networks have been also proposed as attractive targets for applications in organic electronics devices and sensors.[29] For obtaining carbazole-based networks with permanent microporosity, the use of monomers (tectons) with multiple carbazole functions that are arranged around a rigid core unit, as monomers c−f, should be favored.

After initial characterization of the electrochemical behavior of the monomers by cyclic voltammetry, polymer formation was carried out by potentiodynamic electrochemical polymerization of a 0.5 mM solution of the monomers in acetonitrile/dichloromethane (1:4) by using tetrabutylammonium perchlorate (0.1 M TBAP) as supporting electrolyte. A three-electrode cell was used with a platinum disc electrode (1 mm diameter) as WE, a platinum wire as CE, and Ag°/AgNO$_3$ (0.1 M AgNO$_3$, 0.60 V vs NHE) as RE. Finally, the deposited polymer films have been again characterized by cyclic voltammetry.

Figure 1 shows the first oxidation scan for all six monomers. CBPBT, CBP, and SpCz show a first monomer oxidation peak around 0.97 V. The peak current ratio of ca. 2.1 between the
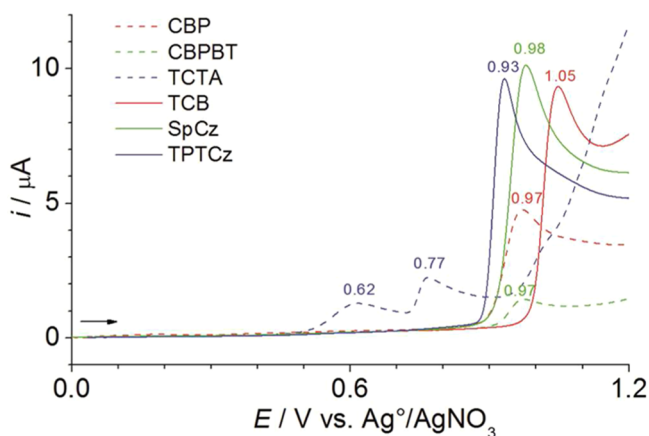
Figure 1. First anodic scan voltammograms for 0.5 mM solutions of the monomers and 0.1 M tetrabutylammonium perchlorate in acetonitrile/dichloromethane (1:4) at a Pt disc electrode. The voltammograms were recorded from 0 to 1.2 V with a scan rate of 0.10 V s^{-1}.

tetra-substituted SpCz and the disubstituted CBP reflects the doubled amount of oxidizable carbazole moieties of SpCz with respect to CBP. A similar ratio is observed for the TPTCz/CBP couple. The low peak current for CBPBT is most probably caused by the low solubility of this monomer; a concentration of 0.5 mM could not be reached in the solvent mixture. For the triphenylamine-cored monomer TCTA, two oxidation peaks at lower potential (0.62 and 0.77 V) are observed during the first cyclovoltammetric scan. This is probably due to the formation of cation radicals and dications of the 1,4-N-substituted phenylene units.[30] The observed shoulder at 1.05 V should correspond to the "regular" carbazole dimerization that is observed for the other five monomers within the potential range of 0.93−1.05 V. Therefore, during subsequent cycling, more complicated voltammograms are observed for TCTA monomer if compared to the well-defined voltammograms that are recorded for the other monomers (see Supporting Information Figure S1). For the other five monomers, starting from the second cycle, one couple of reversible oxidation/reduction peaks is formed in the potential range of 0.5−1.0 V reflecting two electron transfer steps during charging/discharging. Repeated sweeps lead to a progressively increasing peak current, thus reflecting the gradual growth of the MPN films on the electrode. The thickness of the MPN films can be precisely controlled by the cycle number. Cyclic voltammograms of a PTPTCz film on Pt for different scan rates between 0.005 and 0.20 V s^{-1} are depicted in Supporting Information Figure S2. The observed linear relationship between peak current i_p and scan rate v is characteristic for the formation of an electroactive polymer deposit on the electrode.[20] Prolonged potentiostatic electrochemical polymerization of the monomers on ITO allows for the generation of free-standing (TCB, SpCz, and TPTCz) or easily removable (CBP, CBPBT, and TCTA) films due to a reduced adhesion between the ITO electrode and thicker deposits.

Nitrogen gas sorption measurements followed by data analysis using the BET equation belong to the standard techniques for estimating the specific surface area of microporous materials.[31,32] However, this method is not applicable for the precise characterization of materials with very low surface areas or for very small amounts of microporous materials. A way to overcome this problem is to use krypton gas

which has a low saturation pressure of 2.5 Torr at 77 K.[17] For Kr sorption measurements, the MPN films were discharged (dedoped) by applying a potential of 0 V, rinsed with acetonitrile and dichloromethane, removed from the electrode, and dried. The film generation was repeated until ca. 2 mg of material was collected.

For comparison, all monomers were also chemically coupled into bulk MPN powders by oxidative polymerization with FeCl$_3$. The resulting insoluble powders were purified by washing with aqueous concentrated hydrochloric acid, methanol, THF, ethanol, and supercritical CO$_2$ and dried. In the gas sorption measurements, the isotherms show a fast N$_2$ uptake at low pressure (0−0.1 bar), a behavior that is characteristic of permanently microporous materials, with isotherms that are a combination of type I and II behavior[31] (Supporting Information Figure S3). All S_{BET} values are listed in Table 1.

Table 1. Calculated BET Surface Areas of Electropolymerized Films and Chemically Synthesized Bulk MPNs, Using Kr or N$_2$ Gas, Respectively

		S_{BET} (m^2 g^{-1})	
polymer	no. of carbazole units in the monomer	film^a (mean value)	bulk
PCBP	2	76/132 (104)	225
PCBPBT	2	105/213 (159)	324
PTCTA	3	227/239/242 (236)	1065
PTCB	3	652/844 (748)	1647
PSpCz	4	1215/1378 (1297)	1249
PTPTCz	4	1067/1051/1201 (1106)	1322

^{a}Film measurements were carried out at least twice.

The S_{BET} values of films and bulk samples using Kr or N$_2$ gas, respectively, show similar trends within the P/P_0 range of 0−0.6 (Figure 2). Similar S_{BET} values are observed especially for the two tetra-substituted monomers. Very interestingly, a direct relationship between the number of carbazole units of the monomer and the BET surface area of the films is observed. This can be explained by an increased rigidity of the MPNs with increasing cross-linking density, thus leading to an increased permanent microporosity. An unexpectedly low S_{BET} value is observed only for PTCTA. The electrochemical polymerization of monomer TCTA seems problematic due to the presence of the easily oxidizable 1,4-N-substituted phenylene units (see Figure 1), thus causing side reactions and a drastically reduced microporosity of PTCTA. The products made from the bi- and trifunctional monomers CBP, CBPBT, and TCB all show S_{BET} values of thin films that are ca. 50% of the values of the corresponding chemically (FeCl$_3$) synthesized bulk polymers, most probably caused by a reduced cross-linking density during electropolymerization with a preference for the formation of carbazole dimers. Please note that the formation of insoluble MPN films already for the difunctional monomers CBP and CBPBT shows that dimerization is not the only electrochemical process; a certain amount of further couplings of the initially formed dimers occurs. Chemical polymerization with FeCl$_3$ may lead to higher cross-linking densities. For the tetra-functional monomers SpCz and TPTCz the cross-linking density that is obtained by electropolymerization seems high enough to create highly microporous films with BET surface areas in the range of those of the bulk materials, simply as a result of the high functionality of the monomers.
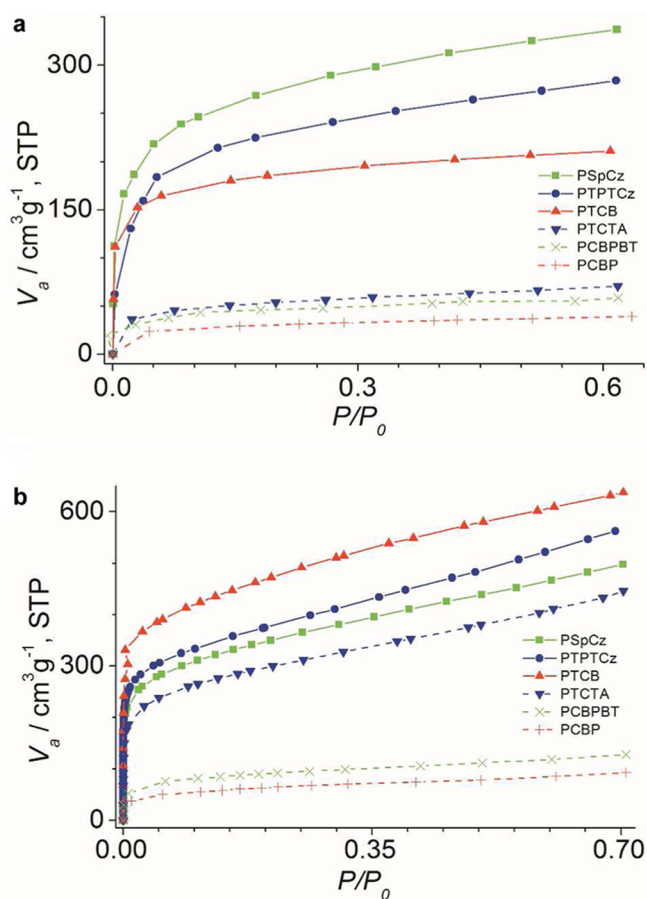
Figure 2. Adsorption isotherms of (a) electropolymerized MPN films and (b) the corresponding bulk polymers made by oxidative coupling with $FeCl_3$, using Kr or N_2 gas, respectively.

aromatic analyte in aqueous solution containing 0.2 M KCl and 0.1 M PBS (pH 7.4).

Linear scan voltammograms (LSV) of 0.5 μM aqueous TNB solutions at MPN-modified and nonmodified GC electrodes are shown in Figure 3a and Supporting Information Figure S5, after
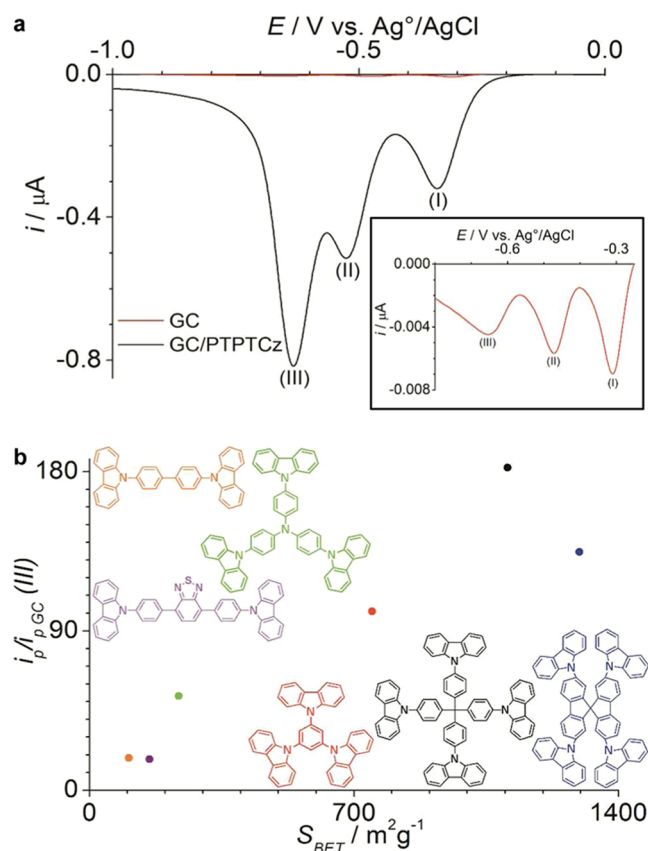

Figure 3. (a) Linear scan voltammograms (after background correction) for nonmodified (inset) and PTPTCz-modified GC electrodes for a TNB concentration of 0.5 μM, and (b) correlation of the current ratios between modified and nonmodified GC electrodes of the third cathodic reduction peak of TNB versus the surface area of the MPN films (scan rate was 0.01 V s^{-1}).

Different meso- and macroporous materials have been used in modified electrodes for the electrochemical detection of nitroaromatic compounds[33−35] driven by the high surface areas of the porous materials as well as molecular interactions between the modified electrodes and the nitroaromatic analytes. To the best of our knowledge, until now MPN films have not been tested in the electrochemical detection of nitroaromatic analytes. Electrochemical studies on the reduction of nitroaromatic compounds in aqueous medium at pH < 9.6 documented the successive formation of nitroso and hydroxylamine functions.[36] Four electrons are transferred in the reduction of a nitro to a hydroxylamine group visible as a single reduction wave.

In our experiments, potentiostatic electrochemical polymerization of the carbazole-based monomers on glassy carbon (GC) electrodes was carried out as first step. The MPN films were produced by applying a potential of 1.1 V until an oxidative charge density of 25.5 mC cm^{-2} was accumulated. So, thin films with a comparable amount of electroactive groups are deposited on the GC electrodes for all monomers (thicknesses between 750 and 900 nm; see Supporting Information Table S1 and Figure S4). After this, the modified GC electrodes were electrochemically discharged (dedoped) and introduced as working electrodes into a three-electrode cell with Ag°/AgCl(sat.) (NaCl 3M, 0.21 V vs NHE) as aqueous reference electrode. The MPN-modified GC electrodes were used for sensing 1,3,5-trinitrobenzene (TNB) as a prototypical nitro-

background correction by subtraction of the reference voltammogram that was recorded in the absence of TNB. Three cathodic peaks for the reduction of the three nitro-substituents of TNB are observed in the voltammograms in the potential range from −0.31 to −0.81 V. For the nonmodified GC electrode, the peaks are observed at −0.31 (I), −0.47 (II), and −0.65 V (III) (see inset of Figure 3a, similar to reported values[37]). The modified GC electrodes show slight shifts of the cathodic potentials dependent on the structure of the monomers used for MPN generation (Supporting Information Figure S5). Interestingly, a dramatic enhancement of the current response is observed for the MPN-modified GC electrodes, 17−182 times higher than the response for the nonmodified electrode (see Supporting Information Table S2). The electrochemical response nicely correlates with the BET surface area of the MPNs (shown for the intensity of the third cathodic peak in Figure 3b). The observed effect may be driven by intermolecular interactions between the high surface of the electron-rich carbazole-based microporous polymer networks and the electron-poor nitroaromatic analytes resulting in a thin adsorbate layer. For mesoporous phorphyrin-based materials
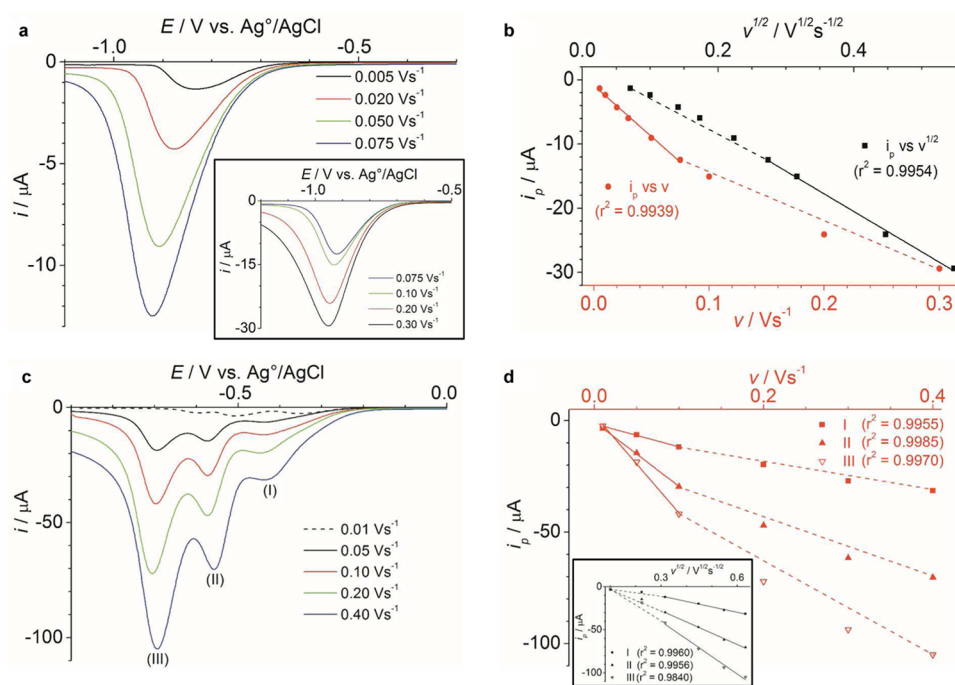
Figure 4. Linear scan voltammograms on PTPTCz-modified GC electrodes for 3.0 μM (a) nitrobenzene (NB) and (c) 1,3,5-trinitrobenzene (TNB) in aqueous 0.2 M KCl and 0.1 M PBS (pH 7.4) solution at scan rates of (a) 0.005−0.075 V s^{-1} (inset: 0.075−0.30 V s^{-1}) and (c) 0.10−0.40 V s^{-1}. Cathodic peak current vs scan rate plots for (b) NB and (d) TNB: linear dependence (red lines) and square root dependence (black lines).

the occurrence of $\pi-\pi$ interactions with NACs has been postulated.[38,39] Our results are also consistent with such an assumption due to the correlation between the surface area of the MPN films and the electrochemical response. The best results are obtained for coatings based on the tetracarbazolyl-substituted monomers that show the highest specific surface areas. PTPTCz-modified GC electrodes show a current ratio of 182 between modified and nonmodified GC electrodes, thus significantly boosting the sensitivity of the electrodes for electrochemical TNB sensing (see Supporting Information Figure S6).

To extract more information about the mechanism of the process, the electrochemical reduction of nitroaromatic analytes at PTPTCz-modified GC electrodes was investigated by linear scan voltammetry at different scan rates. First, Figure 4a shows linear scan voltammograms for 3 μM nitrobenzene (NB) as analyte and scan rates from 0.005 to 0.30 V s^{-1}. For low scan rates (<0.075 V s^{-1}) a negatively shifted asymmetrical wave is observed, characteristic for the irreversible reduction of adsorbed molecules.[40] This behavior is less pronounced for higher scan rates (>0.075 V s^{-1}). Moreover, there is a linear dependence between cathodic peak current and scan rate for low scan rates, as expected for the formation of an adsorbed analyte layer, but a square root dependence for higher scan rates (see Figure 4b). These findings can be interpreted as follows: At low scan rates, the nitrobenzene molecules form a thin adsorbate layer at the MPN surface; an adsorption-controlled process is observed. With increasing scan rate the electron-transfer process becomes diffusion-controlled; since the transport of the nitrobenzene molecules is now the limiting process, the current is now proportional to the square root of the scan rate.

Notably, similar results are also obtained for TNB (Figure 4c,d) and 2,4,6-trinitrophenol (TNP) (Supporting Information Figure S7) independent of their very different solubility in

water. For comparison, similar experiments for nonmodified GC electrodes show the expected linear relationship between peak current and the square root of the scan rate for NB, TNB, and TNP in the scan rate range from 0.01 to 0.4 V s^{-1} (see Supporting Information Figure S8). The obtained linearity indicates a diffusion-controlled process. Regardless of the much higher concentration of the analytes (100 μM) in the experiments with nonmodified GC electrodes (concentration for PTPTCz-modified GC electrodes $\leq$ 3 μM), a higher peak current is observed for the modified electrodes for all nitroaromatic analytes.

■ CONCLUSIONS

In summary, electrochemical polymerization of a series of carbazole-based multifunctional monomers resulted in the generation of microporous polymer networks (MPNs) as thin films with high surface areas up to 1300 m^{2}g^{-1}. The observed porosity is directly related to the number of carbazole units of the monomers. MPN-modified glassy carbon electrodes were successfully used for the electrochemical detection of 1,3,5-trinitrobenzene as prototypical nitroaromatic analyte in aqueous solution, resulting in a distinct enhancement of the cathodic current response by up to 2 orders of magnitude for the best performing microporous polymer network. The electrochemical reduction of the nitroaromatic analytes was found to be an adsorption-controlled process for low scan rates but becomes diffusion-controlled for higher scan rates. Our studies demonstrate a high application perspective of electropolymerized carbazole-based MPN films for the electrochemical sensing of nitroaromatic analytes. Following studies will be focused on a more detailed investigation of the detection scheme, also toward other nitroaromatic explosives and nitroamines.

■ ASSOCIATED CONTENT

Ⓢ Supporting Information

Materials and methods, cyclic voltammograms for the electro-polymerization of the monomers on Pt, nitrogen adsorption–desorption isotherms for the bulk polymers, AFM images of MPN films, including surface roughness and thickness data, detailed electrochemical characterization data for the interaction with nitroaromatic analytes. The Supporting Information is available free of charge on the ACS Publications website at DOI: 10.1021/acsami.5b02233.

■ AUTHOR INFORMATION

Corresponding Author
*E-mail: scherf@uni-wuppertal.de.

Notes
The authors declare no competing financial interest.

■ REFERENCES

(1) Dawson, R.; Stockel, E.; Holst, J. R.; Adams, D. J.; Cooper, A. I. Microporous Organic Polymers for Carbon Dioxide Capture. *Energy Environ. Sci.* **2011**, *4*, 4239−4245.

(2) Fischer, S.; Schimanowitz, A.; Dawson, R.; Senkovska, I.; Kaskel, S.; Thomas, A. Cationic Microporous Polymer Networks by Polymerisation of Weakly Coordinating Cations With CO2-Storage Ability. *J. Mater. Chem. A* **2014**, *2*, 11825−11829.

(3) Chen, Q.; Luo, M.; Hammershøj, P.; Zhou, D.; Han, Y.; Laursen, B. W.; Yan, C.-G.; Han, B.-H. Microporous Polycarbazole with High Specific Surface Area for Gas Storage and Separation. *J. Am. Chem. Soc.* **2012**, *134*, 6084−6087.

(4) Zhang, X.; Lu, J.; Zhang, J. Porosity Enhancement of Carbazolic Porous Organic Frameworks Using Dendritic Building Blocks for Gas Storage and Separation. *Chem. Mater.* **2014**, *26*, 4023−4029.

(5) Zhang, Y.; A, S.; Zou, Y.; Luo, X.; Li, Z.; Xia, H.; Liu, X.; Mu, Y. Gas Uptake, Molecular Sensing and Organocatalytic Performances of a Multifunctional Carbazole-Based Conjugated Microporous Polymer. *J. Mater. Chem. A* **2014**, *2*, 13422−13430.

(6) Zhao, Q.; Zhang, P.; Antonietti, M.; Yuan, J. Poly(ionic liquid) Complex with Spontaneous Micro-/Mesoporosity: Template-Free Synthesis and Application as Catalyst Support. *J. Am. Chem. Soc.* **2012**, *134*, 11852−11855.

(7) Zhang, K.; Kopetzki, D.; Seeberger, P. H.; Antonietti, M.; Vilela, F. Surface Area Control and Photocatalytic Activity of Conjugated Microporous Poly(benzothiadiazole) Networks. *Angew. Chem., Int. Ed.* **2013**, *52*, 1432−1436.

(8) Schmidt, J.; Weber, J.; Epping, J. D.; Antonietti, M.; Thomas, A. Microporous Conjugated Poly(thienylene arylene) Networks. *Adv. Mater.* **2009**, *21*, 702−705.

(9) Bildirir, H.; Paraknowitsch, J. P.; Thomas, A. A Tetrathiafulvalene (TTF)-Conjugated Microporous Polymer Network. *Chem.—Eur. J.* **2014**, *20*, 9543−9548.

(10) Liu, X.; Xu, Y.; Jiang, D. Conjugated Microporous Polymers as Molecular Sensing Devices: Microporous Architecture Enables Rapid Response and Enhances Sensitivity in Fluorescence-On and Fluorescence-Off Sensing. *J. Am. Chem. Soc.* **2012**, *134*, 8738−8741.

(11) Brutschy, M.; Schneider, M. W.; Mastalerz, M.; Waldvogel, S. R. Porous Organic Cage Compounds as Highly Potent Affinity Materials for Sensing by Quartz Crystal Microbalances. *Adv. Mater.* **2012**, *24*, 6049−6052.

(12) Preis, E.; Widling, C.; Scherf, U.; Patil, S.; Brunklaus, G.; Schmidt, J.; Thomas, A. Aromatic, Microporous Polymer Networks with High Surface Area Generated in Friedel-Crafts-Type Poly-condensations. *Polym. Chem.* **2011**, *2*, 2186−2189.

(13) Luo, Y.; Zhang, S.; Ma, Y.; Wang, W.; Tan, B. Microporous Organic Polymers Synthesized by Self-Condensation of Aromatic Hydroxymethyl Monomers. *Polym. Chem.* **2013**, *4*, 1126−1131.

(14) Gu, C.; Chen, Y.; Zhang, Z.; Xue, S.; Sun, S.; Zhang, K.; Zhong, C.; Zhang, H.; Pan, Y.; Lv, Y.; Yang, Y.; Li, F.; Zhang, S.; Huang, F.; Ma, Y. Electrochemical Route to Fabricate Film-Like Conjugated Microporous Polymers and Application for Organic Electronics. *Adv. Mater.* **2013**, *25*, 3443−3448.

(15) Gu, C.; Chen, Y.; Zhang, Z.; Xue, S.; Sun, S.; Zhong, C.; Zhang, H.; Lv, Y.; Li, F.; Huang, F.; Ma, Y. Achieving High Efficiency of PTB7-Based Polymer Solar Cells via Integrated Optimization of Both Anode and Cathode Interlayers. *Adv. Energy Mater.* **2014**, DOI: 10.1002/aenm.201301771.

(16) Zhang, H.; Zhang, Y.; Gu, C.; Ma, Y. Electropolymerized Conjugated Microporous Poly(zinc-porphyrin) Films as Potential Electrode Materials in Supercapacitors. *Adv. Energy Mater.* **2015**, DOI: 10.1002/aenm.201402175.

(17) Gu, C.; Huang, N.; Gao, J.; Xu, F.; Xu, Y.; Jiang, D. Controlled Synthesis of Conjugated Microporous Polymer Films: Versatile Platforms for Highly Sensitive and Label-Free Chemo- and Biosensing. *Angew. Chem., Int. Ed.* **2014**, *53*, 4850−4855.

(18) Dong, W.; Fei, T.; Palma-Cando, A.; Scherf, U. Aggregation Induced Emission and Amplified Explosive Detection of Tetraphenyl-ethylene-Substituted Polycarbazoles. *Polym. Chem.* **2014**, *5*, 4048−4053.

(19) Ma, H.; Yao, L.; Li, P.; Ablikim, O.; Cheng, Y.; Zhang, M. Highly Sensitive and Selective Fluorometric/Electrochemical Dual-Channel Sensors for TNT and DNT Explosives. *Chem.—Eur. J.* **2014**, *20*, 11655−11658.

(20) Wei, Y.; Chan, C. C.; Tian, J.; Jang, G. W.; Hsueh, K. F. Electrochemical Polymerization of Thiophenes in the Presence of Bithiophene or Terthiophene: Kinetics and Mechanism of the Polymerization. *Chem. Mater.* **1991**, *3*, 888−897.

(21) Dietrich, M.; Heinze, J.; Heywang, G.; Jonas, F. Electrochemical and Spectroscopic Characterization of Polyalkylenedioxythiophenes. *J. Electroanal. Chem.* **1994**, *369*, 87−92.

(22) Ribeiro, A. S.; da Silva, A. U.; Ribeiro, L. v. M. O.; da Silva, J. G.; Navarro, M.; Tonholo, J. Electrochemical and Morphological Characterization of Poly[(R)-(−)-3-(1-pyrrolyl)propyl-*N*-(3,5-dinitro-benzoyl)-α-phenylglycinate] Films Deposited on ITO Electrodes. *J. Electroanal. Chem.* **2005**, *580*, 313−319.

(23) Yu, T.; Wu, X.; Lv, Y.; Liu, L.; Du, L.; Zhou, J.; Xie, Z.; Ma, Y. An Electrochemically Deposited Film as an Interface Layer to Improve the Performance of Polymer Light-Emitting Diodes. *J. Mater. Chem. C* **2014**, *2*, 4117−4120.

(24) Groenendaal, L.; Jonas, F.; Freitag, D.; Pielartzik, H.; Reynolds, J. R. Poly(3,4-ethylenedioxythiophene) and Its Derivatives: Past, Present, and Future. *Adv. Mater.* **2000**, *12*, 481−494.

(25) Heinze, J.; Frontana-Uribe, B. A.; Ludwigs, S. Electrochemistry of Conducting Polymers—Persistent Models and New Concepts. *Chem. Rev.* **2010**, *110*, 4724−4771.

(26) Argun, A. A.; Aubert, P.-H.; Thompson, B. C.; Schwendeman, I.; Gaupp, C. L.; Hwang, J.; Pinto, N. J.; Tanner, D. B.; MacDiarmid, A. G.; Reynolds, J. R. Multicolored Electrochromism in Polymers: Structures and Devices. *Chem. Mater.* **2004**, *16*, 4401−4412.

(27) Kerszulis, J. A.; Amb, C. M.; Dyer, A. L.; Reynolds, J. R. Follow the Yellow Brick Road: Structural Optimization of Vibrant Yellow-to-Transmissive Electrochromic Conjugated Polymers. *Macromolecules* **2014**, *47*, 5462−5469.

(28) Ambrose, J. F.; Nelson, R. F. Anodic Oxidation Pathways of Carbazoles: I. Carbazole and N-Substituted Derivatives. *J. Electrochem. Soc.* **1968**, *115*, 1159−1164.

(29) Roncali, J.; Leriche, P.; Cravino, A. From One- to Three-Dimensional Organic Semiconductors: In Search of the Organic Silicon? *Adv. Mater.* **2007**, *19*, 2045−2060.

(30) Chiu, K. Y.; Su, T. X.; Li, J. H.; Lin, T.-H.; Liou, G.-S.; Cheng, S.-H. Novel Trends of Electrochemical Oxidation of Amino-Substituted Triphenylamine Derivatives. *J. Electroanal. Chem.* **2005**, *575*, 95−101.

(31) Sing, K. S. W. Reporting Physisorption Data for Gas/Solid Systems with Special Reference to the Determination of Surface Area and Porosity (Recommendations 1984). *Pure Appl. Chem.* **1985**, *57*, 603−619.

(32) Sing, K. S. W.; Everett, D. H.; Haul, R. A. W.; Moscou, L.; Pierotti, R. A.; Rouquerol, J.; Siemieniewska, T. Reporting Physisorption Data for Gas/Solid Systems. *Handbook of Heterogeneous Catalysis*; Wiley-VCH Verlag: Weinheim, Germany, 2008.

(33) Evans, S. A. G.; Elliott, J. M.; Andrews, L. M.; Bartlett, P. N.; Doyle, P. J.; Denuault, G. Detection of Hydrogen Peroxide at Mesoporous Platinum Microelectrodes. *Anal. Chem.* **2002**, *74*, 1322−1326.

(34) Ma, J.; Zhang, Y.; Zhang, X.; Zhu, G.; Liu, B.; Chen, J. Sensitive Electrochemical Detection of Nitrobenzene Based on Macro-/Meso-Porous Carbon Materials Modified Glassy Carbon Electrode. *Talanta* **2012**, *88*, 696−700.

(35) Qi, B.; Lin, F.; Bai, J.; Liu, L.; Guo, L. An Ordered Mesoporous Carbon/Didodecyldimethylammonium Bromide Composite and Its Application in the Electro-catalytic Reduction of Nitrobenzene. *Mater. Lett.* **2008**, *62*, 3670−3672.

(36) Laviron, E.; Meunier-Prest, R.; Vallat, A.; Roullier, L.; Lacasse, R. The Reduction Mechanism of Aromatic Nitro Compounds in Aqueous Medium: Part II. The Reduction of 4-Nitropyridine between $H_0 = -6$ and pH 9.6. *J. Electroanal. Chem.* **1992**, *341*, 227−255.

(37) Zhang, H.-X.; Cao, A.-M.; Hu, J.-S.; Wan, L.-J.; Lee, S.-T. Electrochemical Sensor for Detecting Ultratrace Nitroaromatic Compounds Using Mesoporous SiO_2-Modified Electrode. *Anal. Chem.* **2006**, *78*, 1967−1971.

(38) Quan, Y.; Xue, Z.; Shi, H.; Zhou, X.; Du, J.; Liu, X.; Lu, X. A High-Performance and Simple Method for Rapid and Simultaneous Determination of Dihydroxybenzene Isomers. *Analyst* **2012**, *137*, 944−952.

(39) Xue, Z.; Lian, H.; Hu, C.; Feng, Y.; Zhang, F.; Liu, X.; Lu, X. Electrochemical Reduction and Detection of Nitrobenzene Based on Porphyrin Composite-Modified Glassy Carbon Electrode. *Aust. J. Chem.* **2014**, *67*, 796−804.

(40) Bard, A. J.; Faulkner, L. R. *Electrochemical Methods: Fundamentals and Applications*, 2 ed.; John Wiley & Sons: New York, 1994.

■ NOTE ADDED AFTER ASAP PUBLICATION

Modifications were made to the version of this paper published May 19, 2015. The corrected version published May 20, 2015.